Size dependence of confined acoustic phonons in CuCl nanocrystals

Jialong Zhao and Yasuaki Masumoto
Institute of Physics, University of Tsukuba, Tsukuba, Ibaraki 305-8571, Japan
(Received 19 March 1999)

Persistent spectral hole burning spectroscopy was used to study the size dependence of the confined acoustic phonons in CuCl nanocrystals embedded in silicate glass, NaCl, and KCl. It is found that the energies of the confined acoustic phonons in the nanocrystals in glass and KCl are almost the same, but twice larger than those in NaCl, which were obtained from the Stokes-side acoustic phonon holes with the same excitation energies. The confined acoustic phonons in the nanocrystals in glass and KCl can be well explained in terms of the lowest-frequency vibrational modes calculated on a sphere model with a free boundary condition. However, the energies of the confined acoustic phonons in the nanocrystals in NaCl are lower than the frequencies of the lowest-frequency vibrational modes predicted by a cube model with a free boundary condition. This observation shows that the energies of the confined acoustic phonons in CuCl nanocrystals depend on the size, the shape, and the boundary condition of the nanocrystals. [S0163-1829(99)13431-3]

Recently, semiconductor nanocrystals have attracted considerable attention from the viewpoint of the fundamental physics and the application possibility to functional devices.[1] In the nanocrystals, not only the electronic energy levels but also the lattice vibrational modes become discrete due to the three-dimensional confinement. The size dependence of electronic and vibrational spectra and the electron-phonon interaction in the nanocrystals is very important for basic understanding of these materials. However, the knowledge on the size dependence of vibrational spectra in the nanocrystals is still in the elementary stage.

Raman scattering is one of the most popular methods to obtain information about the lattice vibrational modes in solids. The low-frequency Raman scattering in the region of several milielectron volts was first observed in $MgCr_2O_4$-$MgAlO_4$ microcrystals by Duval, Boukenter, and Champagnon.[2] After that, similar low-frequency Raman scattering spectra for various nanocrystals such as Ag, CdS, and Si quantum dots were reported by several researchers.[3–7] The frequencies of the low-frequency Raman scattering peaks were found to be inversely proportional to the diameter of the nanocrystal and consistent with those of the low-frequency vibrations of spherical particles predicted by Lamb's theory.[8] Therefore, they were attributed to the confined acoustic phonons in the nanocrystals.[2–7]

The persistent spectral hole burning (PSHB) phenomena have been widely observed in II-VI and I-VII quantum dots and applied to site-selective spectroscopy of quantum dots,[9–12] and, therefore, the PSHB method as a simple method can be used to study the confined acoustic phonons in nanocrystals. CuCl nanocrystals provide a typical example of quantum dots in the weak confinement regime. The narrow homogeneous linewidths of excitons in CuCl nanocrystals in glass and NaCl were observed by using PSHB, transient four-wave mixing, and accumulated photon-echo methods.[13–15] In order to understand their origin and the exciton-phonon interaction with confined acoustic phonons, it is necessary to study systematically the confined acoustic phonons in CuCl nanocrystals. In the previous work,[16] the observation of the confined acoustic phonons in CuCl nanocrystals was reported briefly, but the acoustic phonon sideband holes in CuCl nanocrystals in NaCl were not well distinguished due to the limitation of the spectral resolution.

In this paper, we study in detail the size dependence of the confined acoustic phonons in CuCl nanocrystals in glass, NaCl, and KCl by the PSHB method with improved spectral resolution. Further, we explain the confined acoustic phonons of CuCl nanocrystals in glass, KCl, and NaCl in terms of the lowest-frequency vibrations of the nanocrystals with spherical and cubic shapes, respectively.

CuCl nanocrystals used in the experiment were embedded in sodium aluminoborosilicate glass and NaCl and KCl crystals. The size of the nanocrystals was controlled by heat treatment with different temperature and time. The average size of the nanocrystals was estimated by small-angle x-ray scattering. The samples were directly immersed in superfluid helium at 2 K in an optical cryostat. A narrow-band dye laser pumped by the third harmonics of the output of a Q-switched Nd^{3+}: YAG laser (355 nm) was used as a pump source. The pulse duration and repetition rate were about 5 ns and 30 Hz, respectively. The spectral linewidth was about 0.014 meV. A halogen lamp was used as a probe source. The PSHB spectrum was measured as follows: First, the absorption spectrum was obtained and then the sample was exposed to 9000 shots of dye laser pulses to burn a persistent spectral hole at an excitation energy. The absorption spectral change $-\Delta\alpha d$ is defined as the difference between the spectra before and after the laser exposure. The subsequent measurements were performed at the new position of the samples and were not carried out at the position burnt previously. The transmitted light of the samples was detected by a liquid-nitrogen-cooled charge-coupled device in conjunction with a 75-cm spectrometer involving a 1800 grooves/mm grating operated in the mode of the second order of diffraction. The spectral resolution of the experiment was about 0.13 meV.

Figure 1 shows the absorption (a) and the PSHB spectra (b) of CuCl nanocrystals with an average radius of 1.4 nm in glass at 2 K. The Z_3 exciton absorption band is inhomogeneously broadened due to the size distribution of the nanocrystals. A large blue shift of 64.9 meV is observed in Fig.

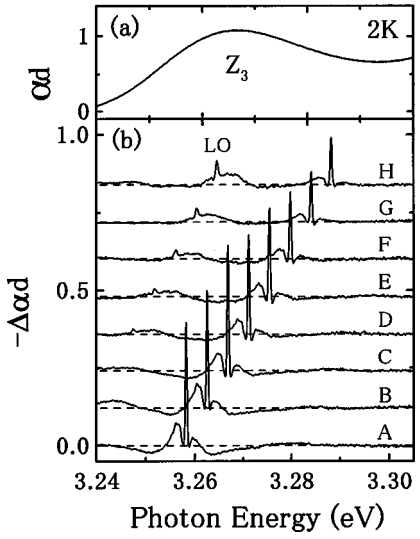

FIG. 1. Linear absorption (a) and the PSHB spectra (b) of CuCl nanocrystals with an average radius of 1.4 nm in glass. The excitation intensity is about 100 nJ/cm^2 and excitation energies for spectra A, B, C, D, E, F, G, and H are 3.2583, 3.2626, 3.2669, 3.2712, 3.2755, 3.2798, 3.2841, and 3.2882 eV, respectively.

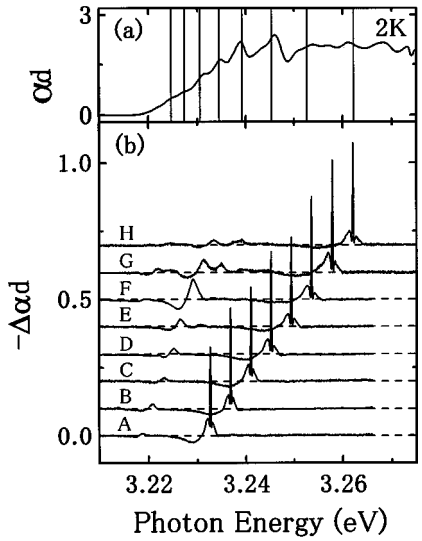

FIG. 2. Linear absorption (a) and the PSHB spectra (b) of CuCl nanocrystals in NaCl. The vertical solid lines in (a) indicate the calculated energies of the Z_3 exciton states under the assumption of a quantum cube. The excitation intensity is about 50 nJ/cm^2 and excitation energies for spectra A, B, C, D, E, F, G, and H are 3.2336, 3.2368, 3.2410, 3.2452, 3.2494, 3.2535, 3.2578, and 3.2621 eV, respectively.

1(a). The vibrational structures in the absorption spectrum of the nanocrystals cannot be distinguished since the Z_3 exciton absorption band is not from the single-sized nanocrystals, but from an ensemble of various sized nanocrystals. As seen in Fig. 1(b), on the other hand, the narrow zero-phonon holes that coincide with the energies of pump beams, and both broad and asymmetric acoustic phonon sideband holes around the zero-phonon line as well as antiholes, are clearly observed. The low-energy side hole is referred to as a pseudophonon wing or a Stokes-side acoustic phonon hole,[10,17] corresponding to the acoustic phonon-assisted absorption of the nanocrystals. The high-energy side one is called a real phonon hole or an anti-Stokes-side acoustic phonon hole, coming from the decrease in the acoustic phonon-assisted absorption of the resonant hole. The interval between the zero-phonon line and the Stokes-side acoustic phonon hole in the PSHB spectra is considered to be the energy of the confined acoustic phonon in the nanocrystal.[16,17] Thus, the energy of the confined acoustic phonon from the Stokes-side acoustic phonon hole in spectrum C in Fig. 1(b) was estimated to be 2.2 meV. By decreasing the nanocrystal size, the confined acoustic phonon energy increases gradually. In addition, a sharp peak with a Stokes shift of about 23.5 meV observed in the PSHB spectra was related to the softened LO phonon.[12]

Figure 2 shows the absorption (a) and the PSHB spectra (b) of CuCl nanocrystals in NaCl at 2 K. Only in NaCl, oscillatory fine structures are observed between 3.22 and 3.28 eV in the inhomogeneously broadened Z_3 exciton absorption band and can be explained by the size-quantized energy states of the Z_3 excitons confined in CuCl quantum cubes whose side changes stepwise in a unit of $a/2$, where a is the lattice constant of the CuCl crystal.[11,18] The vertical solid lines in Fig. 2 indicate the calculated energies of the Z_3 exciton states in the nanocrystals assumed as quantum cubes. There is a well-resolved peak in both Stokes- and anti-Stokes-side acoustic phonon holes when the excitation energy is in the Z_3 exciton absorption band. The energies of the confined acoustic phonons from both holes were estimated to be 0.7 meV at excitation energy of 3.2621 eV and much smaller than those in CuCl nanocrystals in glass and KCl. In addition, the lower-energy satellite holes in the PSHB spectra were supposed to originate from the hole burning of the exciton energy states of CuCl quantum cubes.[11] Here, we must point out that the peaks around the zero-phonon holes in CuCl nanocrystals in NaCl reported in the previous work[16] were from the hole burning of the lowest exciton energy states relaxed from the photoexcited exciton state[11] while the confined acoustic phonon energies were too small to be observed due to the limitation of the spectral resolution.

The PSHB spectra of CuCl nanocrystals with different sizes in glass, NaCl, and KCl were measured systematically to determine the relations between the confined acoustic phonon energy and the size of the nanocrystal as shown in Fig. 3. Both of them were estimated from the Stokes-side acoustic phonon hole at 2 K. The radius and the side length of spherical and cubic CuCl particles in the weak confinement regime[1,11,19,20] were calculated by the confinement energies $E_{Sphere}-E_B=\hbar^2\pi^2/2MR^2$ and $E_{Cube}-E_B=3\hbar^2\pi^2/2ML^2$ assuming that the Stokes-shifted phonon sideband energy coincides with the lowest exciton state energies for spherical and cubic CuCl particles, where E_B is bulk Z_3 exciton energy ($E_B=3.2022$ eV at 2 K), $M=2.3m_0$ is the translational mass of the bulk exciton, and R and L are the radius and the side length of the spherical and cubic nanocrystals, respectively.

The free vibrations of a homogeneous elastic sphere under stress-free boundary conditions were first studied theoretically by Lamb.[8] Two kinds of eigenmodes, the spheroidal and torsional modes, were derived. The eigenmodes are characterized by the angular momentum quantum number l and

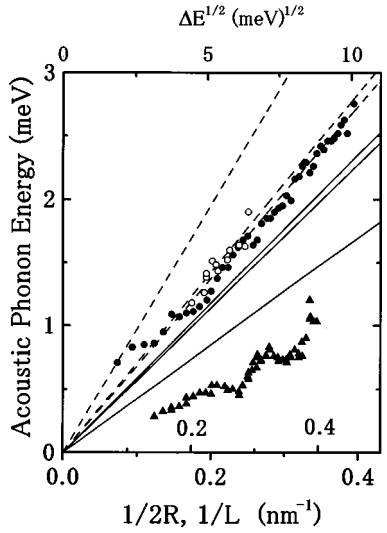

FIG. 3. Confined acoustic phonon energies of CuCl nanocrystals in glass (solid circles), KCl (empty circles), and NaCl (solid triangles) as a function of the size of the nanocrystal. The horizontal axes are drawn in proportion to the inverse of the diameter (the scales below the axis) and the side length (the scales above the axis) of the spherical and cubic nanocrystals, respectively. The upper horizontal axis is drawn in proportion to the square root of the confinement energy. The dashed lines represent the size dependence of the calculated frequencies of the lowest spheroidal ($n=0, l=1$ and $n=0, l=2$) and torsional modes ($n=0, l=2$) of a spherical particle with a free boundary condition, respectively. The solid lines drawn from top to bottom are the results of the theoretical calculation for the lowest torsional, flexural, and shear modes of a cubic particle with a free boundary condition.

branch number n. The longitudinal and transverse sound velocities of bulk CuCl are $v_l=4172$ m/s and $v_t=2021$ m/s derived from the elastic constants[21] $c_{11}=0.72$ and $c_{44}=0.169\times10^{12}$ dyn/cm^2 at 4.5 K and the mass density $\rho=4.136$ g/cm^3. The frequencies of the lowest eigenmodes of a spherical particle are

$$\nu_{10}=1.17v_t/2Rc \quad (n=0,\ l=1,\ \text{spheroidal mode}), \tag{1}$$

$$\nu_{20}=0.82v_t/2Rc \quad (n=0,\ l=2,\ \text{torsional mode}), \tag{2}$$

$$\nu_{20}=0.85v_t/2Rc \quad (n=0,\ l=2,\ \text{spheroidal mode}), \tag{3}$$

where c is the speed of the light in the vacuum. In comparison with the experimental data, the calculated energies of the confined acoustic phonons as a function of the nanocrystal diameter are shown in Fig. 3 with the dashed lines. Figure 3 clearly indicates that the energies of the confined acoustic phonons are inversely proportional to the nanocrystal diameter, which are in good agreement with the frequencies of the lowest-frequency vibrational modes of a spherical particle predicted with Lamb's theory with a free boundary condition. Therefore, we may consider that the shape of CuCl nanocrystals in glass and KCl is spherical and the surface of the nanocrystals is stress-free. In other words, the contact between the nanocrystals and glass and KCl is considered to be weak.

The energies of the confined acoustic phonons of CuCl nanocrystals in NaCl was found to be much smaller than those in glass and KCl obtained with the same excitation energies and can hardly be explained by the elastic sphere model. The previous works have shown that the oscillatory fine structures observed only in the Z_3 exciton absorption band of the nanocrystals in NaCl, the resonantly burned hole, and the lower-energy satellite holes were related to quantum cubes.[11,18] However, the problem of determining the vibration frequencies of a free cube cannot be solved exactly like a free sphere. The free vibrations of an isotropic cube were calculated numerically by Demarest, Jr. using the Rayleigh-Ritz technique.[22] The frequencies of the lowest vibrational modes T_{d1}, F_{a1}, and S_{s1} of a cubic particle are expressed as

$$\nu_{d1}=0.45v_t/Lc \quad (\text{torsional mode}), \tag{4}$$

$$\nu_{a1}=0.59v_t/Lc \quad (\text{flexural mode}), \tag{5}$$

$$\nu_{s1}=0.61v_t/Lc \quad (\text{shear mode}), \tag{6}$$

and are shown in Fig. 3 as the solid lines. Figure 3 shows that the energies of the confined acoustic phonons in CuCl nanocrystals in NaCl are nearer to the frequencies of the vibration mode T_{d1} of a free cube than a free sphere. Thus, the confined acoustic phonons in the nanocrystals in NaCl are rather considered as the lowest-frequency vibrations of cubic nanocrystals, which is in accordance with the previous results.[11,18,23] This shows that the confined acoustic phonon energy is associated with the shape of the nanocrystals in matrices. One can still see the significant discrepancy between the measured and the calculated results. The most possible reason is that an ideal cube with a free boundary condition was simply assumed for the calculation of the frequencies of the confined acoustic phonons of CuCl nanocrystals in NaCl. It is noted that only in NaCl, the orientation of CuCl nanocrystals was demonstrated to be aligned parallel to that of the NaCl crystal by two-photon absorption.[23] The elastic interaction between the nanocrystals and the surrounding lattice was studied and the existence of deformation fields around the nanocrystals was observed by means of a scanning near-field microscope.[24,25] These results show that the surface of CuCl nanocrystals in NaCl is highly strained and the atomic arrangement at the interface between the nanocrystals and the matrix NaCl is more regular than those at the interfaces between the nanocrystals and the surrounding glass and KCl, perhaps resulting in the formation of cubic nanocrystals in NaCl. As a result, CuCl nanocrystals interact with the surrounding NaCl and cannot vibrate freely, similarly to damped oscillators, leading to the softening of the frequencies of the low-frequency vibrations.

The influence of the surrounding matrix on the confined acoustic phonons in nanocrystals have recently been studied by an elastic continuum theory.[26,27] Contradictory conclusions were made. Ovsyuk and Novikov[26] claimed that the matrix effects are important, while Montagna and Dusi[27] reported that the influence of matrices are rather small and can be negligible. In this experiment, the effect of the surrounding matrix on the confined acoustic phonons cannot be observed in the nanocrystals in glass and KCl, but exists in the nanocrystals in NaCl. Therefore, the vibrational frequencies

of the confined acoustic phonons in CuCl nanocrystals depend on the boundary conditions between nanocrystals and matrices.

In summary, we have studied systematically the size dependence of the confined acoustic phonons in CuCl nanocrystals embedded in glass, NaCl, and KCl by the PSHB spectroscopy. The confined acoustic phonons in CuCl nanocrystals in glass and KCl are explained as the lowest-frequency vibrations of the spherical nanocrystals with the free boundary condition. Those in CuCl nanocrystals in NaCl are explained as the softened lowest-frequency vibrations of the cubic nanocrystals with the strained boundary condition.

We would like to thank Dr. T. Mishina, Dr. T. Okuno, Dr. J. Qi, and Dr. M. Ikezawa for valuable discussions. This work was partially supported by the Scientific Research Grant-in-Aid No. 10554011 from the Ministry of Education, Science, Sports, and Culture of Japan. Small angle x-ray scattering experiments were done in the Photon Factory of the National Laboratory for High-Energy Physics (98G071).

[1] U. Woggon, *Optical Properties of Semiconductor Quantum Dots* (Springer, Berlin, 1997).
[2] E. Duval, A. Boukenter, and B. Champagnon, Phys. Rev. Lett. **56**, 2052 (1986).
[3] M. Fujii, T. Nagareda, S. Hayashi, and K. Yamamoto, Phys. Rev. B **44**, 6243 (1991).
[4] A. Tanaka, S. Onari, and T. Arai, Phys. Rev. B **47**, 1237 (1993).
[5] L. Saviot, B. Champagnon, E. Duval, and A. I. Ekimov, Phys. Rev. B **57**, 341 (1998).
[6] M. Fujii, Y. Kanzawa, S. Hayashi, and K. Yamamoto, Phys. Rev. B **54**, R8373 (1996).
[7] F. Q. Liu, L. S. Liao, G. H. Wang, G. X. Cheng, and X. M. Bao, Phys. Rev. Lett. **76**, 604 (1996).
[8] H. Lamb, Proc. London Math. Soc. **13**, 189 (1882).
[9] K. Naoe, L. G. Zimin, and Y. Masumoto, Phys. Rev. B **50**, 18 200 (1994).
[10] Y. Masumoto, K. Sonobe, and N. Sakakura, J. Lumin. **72-74**, 294 (1997).
[11] N. Sakakura and Y. Masumoto, Phys. Rev. B **56**, 4051 (1997).
[12] L. Zimin, S. V. Nair, and Y. Masumoto, Phys. Rev. Lett. **80**, 3105 (1998).
[13] Y. Masumoto, T. Kawazoe, and N. Matsuura, J. Lumin. **76-77**, 189 (1998).
[14] R. Kuribayashi, K. Inoue, K. Sakoda, V. A. Tsekhomskii, and A. V. Baranov, Phys. Rev. B **57**, R15 084 (1998).
[15] M. Ikezawa and Y. Masumoto (unpublished).
[16] S. Okamoto and Y. Masumoto, J. Lumin. **64**, 253 (1995).
[17] J. Friedrich, J. D. Swalen, and D. Haarer, J. Chem. Phys. **73**, 705 (1980).
[18] T. Itoh, S. Yano, N. Katagiri, Y. Iwabuchi, C. Gourdon, and A. I. Ekimov, J. Lumin. **60-61**, 396 (1994).
[19] A. L. Efros and A. L. Efros, Fiz. Tekh. Poluprovodn. **16**, 1209 (1982) [Sov. Phys. Semicond. **16**, 772 (1982)].
[20] T. Itoh, Y. Iwabuchi, and M. Kataoka, Phys. Status Solidi B **145**, 567 (1988).
[21] *Physics of II-VI and I-VII Compounds, Semimagnetic Semiconductors*, edited by O. Madelung, M. Schulz, and H. Weiss, Landolt-Börnstein, New Series, Group III, Vol. 17, Pt. b (Springer, Berlin, 1982).
[22] H. H. Demarest, Jr., J. Acoust. Soc. Am. **49**, 768 (1971).
[23] D. Fröhlich, M. Haselhoff, K. Reimann, and T. Itoh, Solid State Commun. **94**, 189 (1995).
[24] H.-J. Weber, K. Lüghausen, M. Haselhoff, and H. Siegert, Phys. Status Solidi B **191**, 105 (1995).
[25] A. Diegeler, M. Haselhoff, W. Rammensee, and H.-J. Weber, Solid State Commun. **105**, 269 (1998).
[26] N. N. Ovsyuk and V. N. Novikov, Phys. Rev. B **53**, 3113 (1996).
[27] M. Montagna and R. Dusi, Phys. Rev. B **52**, 10 080 (1995).